

**H14-158**  
**LES OF COHERENT STRUCTURES IN A STREET CANYON**

*Vladimir Fuka<sup>1</sup> and Josef Brechler<sup>1</sup>*

<sup>1</sup>Department of Meteorology and Environment Protection, Faculty of Mathematics and Physics, Charles University in Prague, Czech Republic

**Abstract:** This study presents results of computer simulation of flow over a series of street canyons. The setup is taken from an experimental study by Kellnerová et al. (2010). The problem is simulated by an LES model CLMM (Charles University Large Eddy Microscale Model). The results are analysed using proper orthogonal decomposition and spectral analysis.

**Key words:** *street canyon, large eddy simulation, proper orthogonal decomposition*

## INTRODUCTION

The coherent structures in the turbulent flow can carry substantial part of turbulent kinetic energy (TKE) and determine the form of the flow. The repeating features of the flow with high TKE can be examined by the proper orthogonal decomposition (POD) (Sirovich, 1987). The inputs for the analysis are time and space dependent fields of the variables (e.g. wind velocity). The decomposition is performed on series of snapshots of the flow. The fields can be result of measurement or simulation.

An experimental study by Kellnerová et al. (2010) studied flow in a series of parallel street canyons. This paper presents computation of a similar setup. The main difference is the cyclic inflow and outflow condition used for the simulation.

## NUMERICAL MODEL

The simulations were performed using the model CLMM (Charles University Microscale Model; Fuka and Brechler, 2010) which solves the incompressible Navier-Stokes equations using large eddy simulation (LES). The equations are solved on a staggered orthogonal grid. The projection method is used to couple the momentum equations and the continuity equation. The Vreman (2004) model is used as a closure for computation of the subgrid stresses. It is an algebraic eddy viscosity model which does not suffer from excessive dissipation in laminar areas and near solid walls. Because of the orthogonal grid the immersed boundary method is used to enforce the correct geometry of the obstacles (Kim et al., 2001, Bodnár et al. 2008). The subgrid stresses near solid walls were computed by a wall model using the wall function approach.

## SIMULATED PROBLEM

The experimental setup in study by Kellnerová et al. (2010) consisted of a square wind channel 25 × 25 cm in cross-section approximately 3 m long with a series of parallel street canyons with two types of buildings. The first building shape was a building with a flat roof  $H = 5$  cm wide and high. The other type had pitched roof that was made by cutting the first type of building at 3 cm height. The street was 5 cm wide in both cases. The geometry is apparent from figures in the following parts.

In our simulation we used a 2 m long domain with the same cross-section and building dimensions, i.e. we had 20 parallel buildings in the domain. For the inflow and outflow we used cyclic boundary conditions. That means we had periodic row of 20 street canyons.

The flow was driven by a constant pressure gradient that was kept the same value in both cases. That caused a little difference in the wind speed in the centre of the channel. The maximum time-averaged wind speed in the channel with the flat roof was 6.2 ms<sup>-1</sup>, whereas for pitched roofs it was 5.2 ms<sup>-1</sup>.

The simulation was carried out on a uniform grid with 640 × 97 × 97 control volumes. We also performed simulations with shorter domain, but the flow was then dominated by a wave with the wavelength equal to the length of the domain.

## PROPER ORTHOGONAL DECOMPOSITION

The proper orthogonal decomposition is a method for getting a new orthogonal basis of the state space, in which the individual base vectors (so called modes) explain largest possible part of the variability of the time dependent system. The state of the system in each time can be written as a linear combination of the modes

$$q_j - \bar{q} = \sum_k c_{jk} \varphi_k \quad (1)$$

where  $q_j$  are snapshots of the state vector at different times,  $\bar{q}$  is the average state,  $\varphi_k$  are the POD modes and  $POD$  coefficients. The modes are solution to an optimization problem, to maximize a functional

$$\max_{q_1, \dots, q_l} \sum_{i=1}^l \sum_{j=1}^n \left| \langle q_j, \varphi_i \rangle \right|^2 \quad \text{such that} \quad \langle \varphi_i, \varphi_j \rangle = \delta_{ij}. \quad (2)$$

In the context of turbulent flow we can interpret POD modes with lower index also as structures containing the most of turbulent kinetic energy (TKE). We used Fortran program SVD\_BASIS by John Burkhardt to solve (2). It is based on singular value decomposition (SVD) (Burkhardt et al., 2006).

## RESULTS

We computed 10 s of flow in both geometrical configurations and used last seven seconds to gain snapshots and other statistics. The average flow in the both types of street canyon is in Fig. 1. We stored 10000 2D snapshots of the flow (all three velocity components) at the central plane  $xz$ . We computed the POD modes on a section of the plane covering a close proximity of one selected canyon. The first 3 modes for the pitched roofs case are plotted in Fig. 2. They have a similar shape to those computed by Kellnerová et al. from their PIV measurements. Regrettably, at the time of writing, we didn't have access to the exact numerical data from the experiment yet.

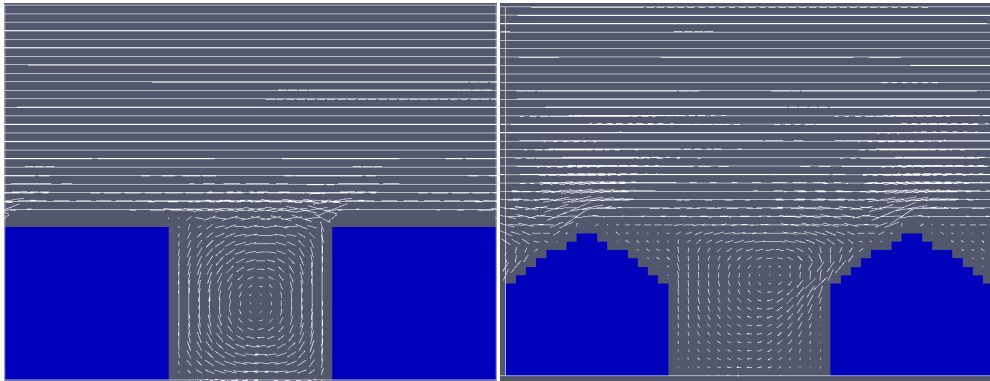


Figure 1. The time averaged flow in the flow canyon for the flat roofs (left) and the pitched roofs (right).

From the computed flow field itself, and also from the POD analysis, it was clear that the flow is more complex in the case of pitched roofs. In the case of flat roofs the vortices separated at the lee side of the building continue mostly directly to the edge of the building and form a quasi-steady shear layer at the top of the canyon. Also the main vortex in the street canyon itself is more stable and is well pronounced almost at all times. This is not true in the case of pitched roofs where a recirculation zone behind upwind building's roof forms but is not totally stable. The vortices detached from the top edge of the building continue in different directions and impinge on the next building in different positions or even continue above it. These findings are consistent with the findings of Kellnerová et al. The following analysis will mostly concern pitched roofs.

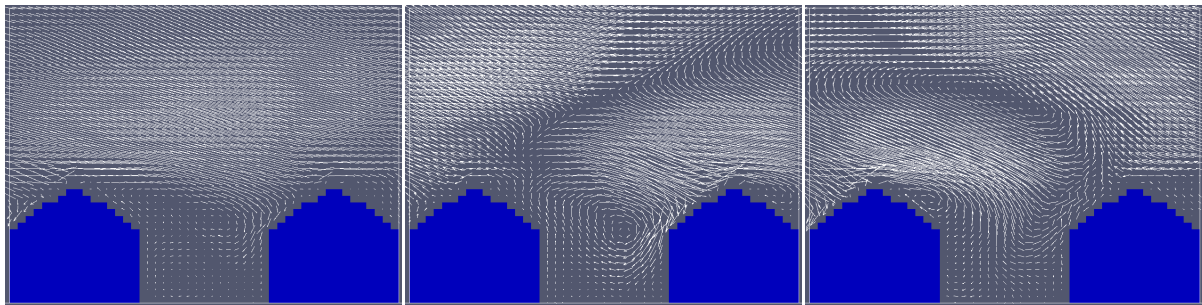


Figure 2. The first 3 POD modes for the pitched roofs.

We also performed Fourier spectral analysis of the velocity component time series in the middle of the canyon at the roof level height. The spectra are plotted in Fig. 3. There is a very obvious distinction between the two roof shapes. For the flat roofs, the inertial range is not well developed. The possible cause of this is the fact that the inertial range begins at higher frequencies, which are close to the subgrid scale. Also turbulence in the canyon is very far from theoretical case with Taylor frozen turbulence hypothesis. In the case of pitched roofs, the spectra show a clear inertial range between approximately 10 Hz and 200 Hz. The high frequency end of the resolved inertial range is caused by limited resolution. The present grid cannot resolve motions smaller than 6 mm and the spatial scale and time scale of turbulence are closely connected. The low dominating frequencies of the flow are probably affected by the cyclic boundary conditions which prefer frequencies that are a multiple of the mean advection velocity above the roof level which is roughly  $5.6 \text{ ms}^{-1}$  for flat roofs and  $4.5 \text{ ms}^{-1}$  for pitched roofs divided by the domain length (2 m).

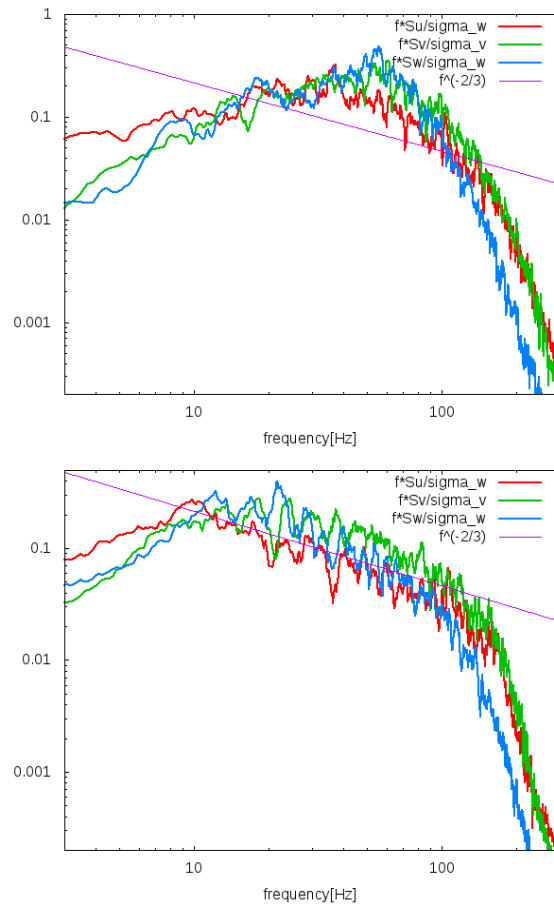


Figure 3. The (filtered) spectra of velocity components at the centre of the channel at the height  $z=H$  for flat roofs (left) and pitched roofs (right).

Another task performed was to compute the Fourier spectra of the POD coefficients of first three modes (Fig. 4). They contain less high frequency parts, than velocity components themselves, as expected. Some of the peaks are common among the modes, but the first mode contains considerably more low frequencies. The same argument about spoiling the frequency spectrum because of the boundary conditions applies here. The coherence of the modes can be seen in a better way by the cross correlation functions in Fig. 5. The peaks in cross correlation between first four consecutive modes are above 0.4 and in the case of correlation between modes 3 and 4 above 0.5. This means that the POD modes are not independent in their dynamics. In the graph of time series of the coefficients in Fig. 6 one can see that the peaks of mode 1 coefficient are often followed by the peak of mode 2. This feature was also found in experiment and Kellnerová et al. interpret this as the mode 1 bringing more kinetic energy to the canyon by strengthening the recirculation behind the upwind roof and the mode 2 responding by strengthened main vortex. For the other consecutive modes, the cross-correlation is opposite, i.e. the mode with lower number is lagged behind the mode with higher number.

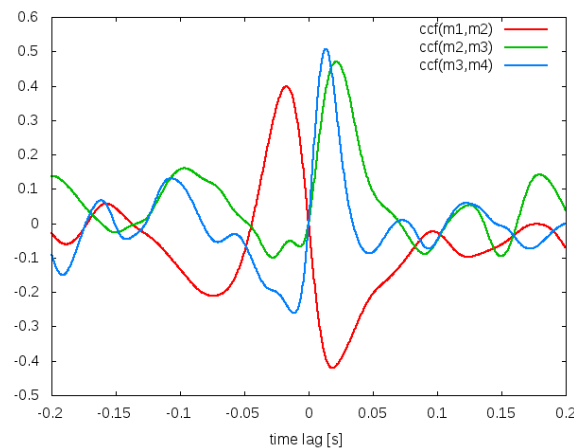


Figure 5. The cross correlation functions between the first four consecutive POD modes for pitched roofs.

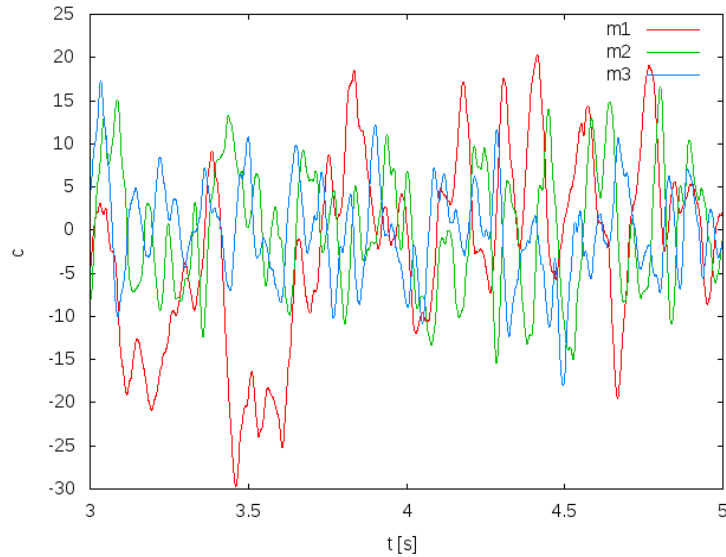


Figure 8. A part of the time series of POD coefficients for first 3 modes for pitched roofs.

The spanwise velocity fluctuations form interesting features of the flow, that couldn't have been measured in the wind channel unfortunately. In our simulations they produce ramp like features with dimension comparable to the building dimension, so that they are the prevailing coherent structures above the canopy. A typical example of their appearance is in Fig. 7. Unfortunately the blockage by the upper wall of the channel is likely to affect them a lot, because they tend to protrude high in the inertial layer. Finally, in Fig. 8 the vortical structures in the flow are visualized using the  $\lambda_2$  criterion. They tend to dominate the flow above the canopy. Because they are smaller in size than the structures of spanwise velocity, they are probably somehow organized but this has not been investigated yet.

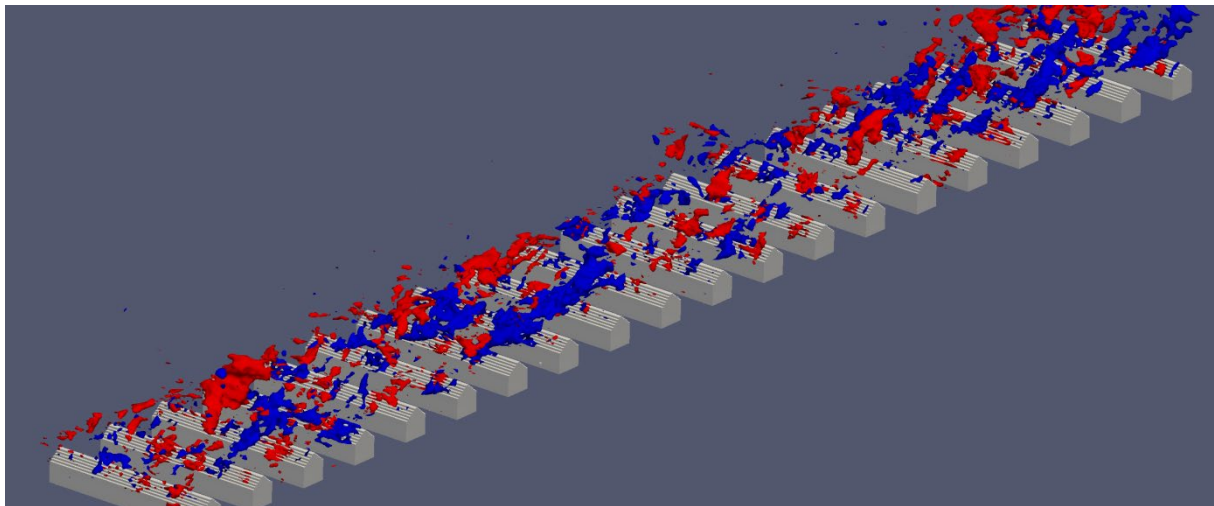


Figure 7. The isocontours of spanwise velocity component  $-1 \text{ ms}^{-1}$  (blue) and  $+1 \text{ ms}^{-1}$  (red).

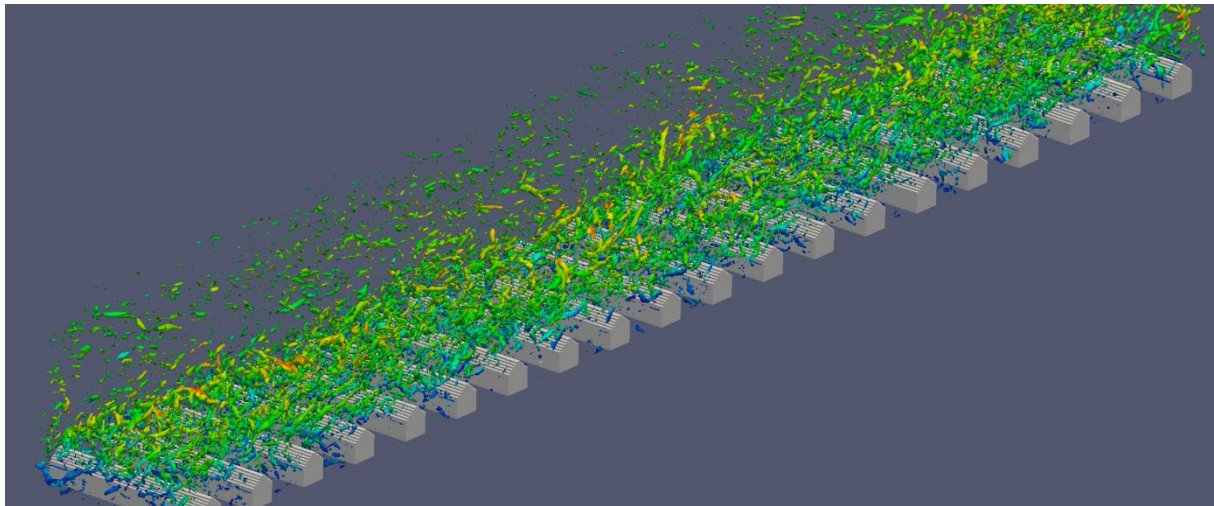


Fig. 8. The turbulent vortices visualised using the  $\lambda_2$  criterion.

## CONCLUSIONS

We performed a large eddy simulation of the flow in a channel with parallel street canyon based on an experiment. We were able to compare only qualitative agreement between our results and experiment. Probably a higher resolution should be desired as we had only 16 grid cells in the street canyon. With our present hardware we would have to sacrifice number of the canyons in the periodic domain, which would lead to strong limitation of reliability of the spectral properties of the flow. The flow in the canyon itself seems not to be affected by domain length so much in our preliminary tests. We are preparing computations with free top boundary condition positioned higher above the buildings to assess the effect of blockage. This computation will also include dispersion of a top-down and bottom-up scalar for direct evaluation of scalar fluxes and the role of street canyon shape for its ventilation.

## ACKNOWLEDGMENTS

The work was supported by the Czech Ministry of Education, Youth and Sports under the framework of research plan MSM0021620860.

## REFERENCES

- Bodnár T., Beneš L., Kozel K., 2008: Numerical simulation of flow barriers in complex terrain. *Nuovo Cimento Della Societa Italiana Di Fisica C* 31, pp. 619-632.
- Burkardt J., Gunzburger M., Lee H.-C., 2006: Centroidal Voronoi Tessellation-Based Reduced-Order Modelling of Complex Systems, *SIAM Journal on Scientific Computing*, Volume 28, Number 2, pages 459-484.
- Kellnerová R., Kukačka L., Uruba V., Antoš P., Odin J., Jaňour Z., 2010: Wavelet and POD Analysis of Turbulent Flow Within Street Canyon. *Experimental fluid mechanics* 2010. Jičín (Czech Republic).
- Kim J., Kim D., Choi H., 2001: An Immersed-Boundary Finite-Volume Method for Simulations of Flow in Complex Geometries. *J. Comp. Phys.* 171. pp. 132-150.
- Sirovich L., 1987: Turbulence and dynamics of coherent structures. Part I: coherent structures. *Q. Appl. Math.* 45. pp. 561-571.
- Vreman, A., 2004: An eddy-viscosity subgrid-scale model for turbulent shear flow: Algebraic theory and applications, *Phys. Fluids* 16. pp. 3670-3681.